*Desalination and Water Treatment*
www.deswater.com

doi: 10.1080/19443994.2015.1005692

57 (2016) 5398–5405
March

Taylor & Francis
Taylor & Francis Group

# Theoretical estimation of semi-permeable membranes leading to development of forward osmosis membranes and processes as a future seawater desalination technology

Yuya Sato[a,*], Shin-ichi Nakao[b]

[a]*AR-2 Lab, Samsung R&D Institute Japan, Yokohama 2300027, Japan, Tel. +81 45 510 3971; email: y.sato@samsung.com*
[b]*Faculty of Engineering, Department of Environmental and Energy Chemistry, Kogakuin University, 2665-1 Nakano, Hachioji 1920015, Tokyo, Japan, Tel. +81 42 628 4542; email: maku@cc.kogakuin.ac.jp*

Received 3 July 2014; Accepted 26 December 2014

ABSTRACT

Recently, forward osmosis (FO) process has been expected for the future seawater desalination method. In this study, the estimation of semi-permeable membranes leading to development of FO membranes and processes was investigated from the theoretical calculation view point. It is common to apply multivalent ionic materials to draw solution in FO membrane process. $MgCl_2$, one of the common multivalent ionic materials, was used for calculating the relationship between pure water permeability (A value) and required FO membrane length. Two cases were assumed—one as an ideal condition which was without any concentration polarization (CP), the other as an actual condition which was with external concentration polarization. In the case of non-CP condition, the membrane length decreased with increase the A value. On the other hand, in the case of CP condition, the membrane length converged to constant value with increase of the A value. From this phenomenon, there was the optimized relationship between A value and membrane length. For instance, under the condition of $MgCl_2$ concentration at 12.9 wt%, the A value over $2.0 \times 10^{-11}$ [$m\,s^{-1}\,Pa^{-1}$] was required while the membrane length was equal to eight elements. Moreover, the effect of mass transfer coefficient was estimated. It was suggested that the estimation was possible for the A value and the membrane length with any given mass transfer coefficients.

*Keywords:* Forward osmosis; Desalination; Semi-permeable membrane; Concentration polarization; Pure water permeability

## 1. Introduction

It has been claimed that the situation of the water shortage issues in the world is becoming more serious these days. The number of seawater desalination plants has been increasing year-by-year especially in the Middle East, which has big problems with drinking water. There are two well-known seawater desalination methods—evaporation and reverse osmosis (RO) processes. Recently, the number of RO plants has increased drastically for seawater desalination as an energy saving method without phase change [1]. The so-called "water business" is expanding and the market size expected for 2025 is about 87 trillion yen,

*Corresponding author.

that is about triple compared to 2007 [2,3]. Water treatment field is very attractive not only for business but also for technology, research and development.

Recently, a forward osmosis (FO) process has been expected to have a high potential for the future seawater desalination mainly as a further energy saving method [4,5]. FO process mechanism is based on an osmotic pressure (OP) differential across a semi-permeable membrane. The driving force of OP is only based on concentration differences across a membrane, which requires little hydraulic pressure, so the energy consumption of water separation with an FO membrane is theoretically zero in the ideal condition. Actually, the total process with FO membranes for seawater desalination requires some energy such as the supplying energy of seawater and draw solution (DS) to FO membranes and the water recovering energy from DS to gain freshwater. However, along with the innovations of suitable DS and water recovery systems, the desalination process with FO membranes still has an enormous potential in reducing energy consumption compared to RO process [6,7].

Only a few actual plants with FO process are in operation now. FO pilot plant in Oman installed by Modern Water plc, the pioneer company in this field, may be only case [8,9]. In addition, variety of commercial FO membrane is limited. Hydration Technology Innovations may be the only company producing the commercial FO membranes [10]. Commercial RO membranes can be used for experiments instead of FO membranes because of their semi-permeability [11,12].

Although OP is the traditional well-known natural principle, the research of FO method as a seawater desalination process is relatively young [13]. Extensive studies have been conducted on FO membranes and processes by many researchers nowadays. The key factors of the FO method as a seawater desalination may be (1) an FO membrane, (2) DS, (3) a water recovery system, and (4) a total process. There are a number of researches developing the new FO membrane itself and also various approaches exist [14–17]. Though, most of them are mainly aiming only to develop FO membranes and measuring the basic performances such as pure water permeability (A value). The current level of these FO membranes' A values is around $10^{-12}$ to $10^{-11}$ [$m\,s^{-1}\,Pa^{-1}$]. These values may not be enough for actual FO membranes, so further improvement will be required. There are also a number of researches developing the new DS such as multivalent ionic materials [18,19] and ammonia–carbon dioxide [20,21], with their own FO processes. However, almost all of them adopted commercial FO membranes, and the membranes and processes are not always optimized.

To put the FO method into a practical seawater desalination usage, it is obvious that the design of suitable FO membranes and processes is one of the important factors. Examination of FO membranes' characteristics, that is to say, required A values and number of elements, are very significant to build the system.

The objective of this study is establishment of the design direction for FO membranes (A values) and processes in seawater desalination plants. The estimation of semi-permeable membranes leading to development of FO membranes and processes was investigated from the theoretical calculation view point. Required plant scale was estimated by the relationship between A values and recovery rates of FO membranes in this paper.

## 2. Theory

The transport phenomena in membrane processes can be described by the classical solution-diffusion model [22].

$$J_V = A \cdot (\Delta P - \Delta\pi) \tag{1}$$

$$J_S = B \cdot (C_m - C_P) \tag{2}$$

where $J_V$ and $J_S$ are the volumetric flux and the solute flux. A and B are the transport parameters known as the pure water permeability and the solute permeability, respectively.

In an FO membrane, the driving force is OP differential, so the Eq. (1) can be described as follows:

$$J_V = A \cdot (\pi_D - \pi_F) \tag{3}$$

where $\pi_D$ and $\pi_F$ are the OP at DS side and feed side.

The external concentration polarization (ECP) at both DS and feed side can be described as:

$$\frac{C_{Dm}}{C_{Db}} = \exp \cdot \left( -\frac{J_V}{k_D} \right) \tag{4}$$

$$\frac{C_{Fm}}{C_{Fb}} = \exp \cdot \left( \frac{J_V}{k_F} \right) \tag{5}$$

From the definition of the Sherwood number:

$$Sh = \frac{kd}{D} \tag{6}$$

and the mass transfer coefficient is calculated as

$$k = \frac{Sh \cdot D}{d} \tag{7}$$

In this study, it is assumed to use spiral wound FO elements. From the calculation based on the linear velocity, the Reynolds number is in the range of laminar flow, however, the flow will be a turbulent flow in actual because of the feed spacer effect. Deissler's equation can be generally used in the range of turbulent flow [23–25];

$$Sh = 0.023 \cdot Re^{0.875} \cdot Sc^{0.25} \tag{8}$$

However, this equation does not consider the effect of feed spacer. In this study, the empirical equation based on the experiments with spiral wound elements will be applied [26].

$$Sh = 0.065 \cdot Re^{0.875} \cdot Sc^{0.25} \tag{9}$$

The definitions of the Schmidt number and Reynolds number are given by

$$Re = \frac{\rho u d}{\mu} \tag{10}$$

$$Sc = \frac{v}{D} \tag{11}$$

At the high concentration range, the OP is not proportional to the concentration [13]. This study does not include the accurate calculation of OP from the concentration. Thus, in this study, it is assumed that the OP can be calculated by the van't Hoff equation to simplify the calculation.

$$\pi = \frac{nRT}{V} \tag{12}$$

## 3. The calculation conditions

In this paper, the calculation has proceeded assuming two conditions: (1) without any CP which is an ideal condition and (2) with external CP which is an actual condition. Fig. 1 describes the concentration profiles of the solutions across an FO membrane. It is well known that thin film composite membranes are affected by two sorts of CPs—one is the ECP at outside of a membrane, the other is the internal concentration polarization (ICP) at inside of a support layer. Some studies reported that ICP might affect more on membrane permeability compared to ECP and reducing the driving force given by OP differential [27,28], which means it is impossible to avoid the ICP effect. However, those kinds of studies have done only with the commercial RO and FO membranes, and in order to apply an FO membrane method to a practical use, what really required is the technological innovation to reduce the ICP effect as low as possible. For example, it can be an innovated support layer which raises huge turbulent flow inside of itself, it can be an innovated FO membrane without any support layers ultimately, etc.

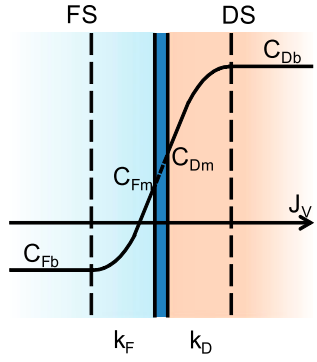


Fig. 1. The concentration profiles of the solutions across an FO membrane.

From these points of view, ICP is not considered in this paper with the expectation of future actual innovation. The calculation method which includes ICP effect and new materials to reduce ICP is now on process, and it will be reported in near future. Moreover, in this study, the FO membrane is ascribed to

Table 1
The parameters for the calculation

| | | |
|---|---|---|
| The height of FS side ($h_F$) | [m] | $1.0 \times 10^{-3}$ |
| The height of DS side ($h_D$) | [m] | $1.5 \times 10^{-3}$ |
| FO membrane element width | [m] | 1.0 |
| FO membrane element length | [m] | 1.0 |
| Initial linear velocity of FS | [m $s^{-1}$] | $1.25 \times 10^{-1}$ |
| Initial linear velocity of DS | [m $s^{-1}$] | $1.25 \times 10^{-1}$ |
| The concentration of FS (NaCl) | [wt%] | 3.5 |
| Molecular weight (NaCl) | [g $mol^{-1}$] | 58.5 |
| Molecular weight ($MgCl_2$) | [g $mol^{-1}$] | 95.3 |
| Mass transfer coefficient (NaCl)[a] | [m $s^{-1}$] | $3.52 \times 10^{-5}$ |
| Mass transfer coefficient ($MgCl_2$)[a] | [m $s^{-1}$] | $2.76 \times 10^{-5}$ |
| Temperature of the solution | [K] | 298 |

[a]Calculated by Eq. (7).

Table 2
The osmotic pressure and optimized values for each concentration of $MgCl_2$

| Concentration [wt%] | Osmotic pressure[a] [MPa] | A value [$m\,s^{-1}\,Pa^{-1}$] | The number of membranes [–] | Maximum recovery rate [%] |
|---|---|---|---|---|
| 12.9 | 10 | $2.0\times10^{-11}$ | 8 | 39 |
| 14.1 | 11 | $3.0\times10^{-11}$ | 7 | 41 |
| 15.4 | 12 | $2.0\times10^{-11}$ | 7 | 43 |
| 16.7 | 13 | $3.0\times10^{-11}$ | 6 | 45 |
| 18.0 | 14 | $3.0\times10^{-11}$ | 6 | 46 |

[a]Calculated by Eq. (12).

have perfect rejection, that is, no solutes can pass through the FO membrane. The effect of the solute permeability (B value) is now under consideration.

The parameters for the calculations are listed in Table 1. The height and initial linear velocity of FS side and membrane sizes are based on the design of commercial RO membranes such as FILMTEC™ SW30HRLE and usual operating conditions. The height of DS side is assumed to be 1.5 times larger than that of FS side in this calculation, since the DS volume increases along with the flow direction. Initial linear velocity of DS is supposed to be equal to that of FS in this study. These parameters can be fixed when the module structure is completely designed. Mass transfer coefficients are calculated by Eq. (7). It is common to apply multivalent ionic materials to DS in FO membrane process. $MgCl_2$, one of the common multivalent ionic materials, is used for this calculation. The required membrane length is estimated to achieve the recovery rate of 30, 35, and 40% with each concentration shown in Table 2. The membrane length represents the number of the FO membrane elements, in other words, the scale of FO plant. The relationship between A values and maximum recovery rates with each concentration and membrane length is investigated. In addition, in the case of other DS except for $MgCl_2$, the effect of mass transfer coefficient is estimated to generalize this study method—the number of required FO elements is calculated by varying the mass transfer coefficient of the DS ($k_D$).

The structure of FO elements has not been standardized even in the world. Fig. 2 describes one example of the structure [13,28,29]. The blocking at the middle of the central tube and glue line lets the DS flow to be like a shape of "U". However, additional improvement might be required to obtain the stable flow. In this paper, it is assumed that both the feed and the DS are in parallel flow as shown in Fig. 3. The counter-flow system, which is more efficient for the FO system, and the cross-flow system are now under consideration.

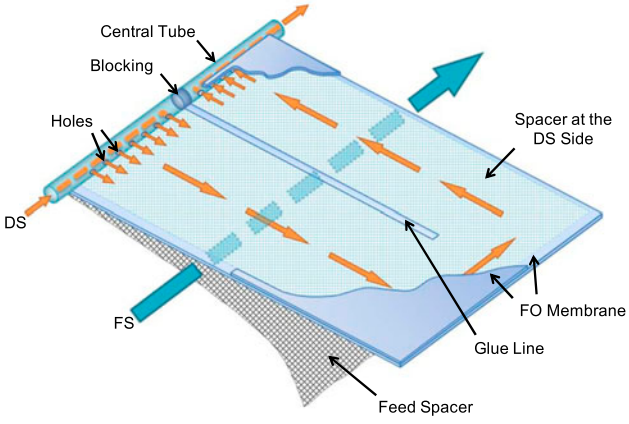


Fig. 2. The common structure of a spiral wound FO module as an example.

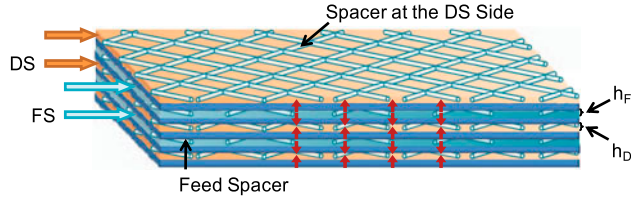


Fig. 3. The schematic image of parallel flow for the calculation.

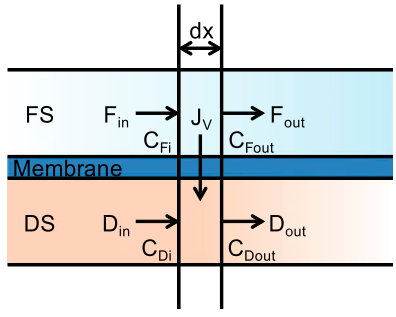


Fig. 4. The illustration of the calculation concept in this study.

The calculation concept is described in Fig. 4. The amount of water permeation from the feed side to the DS side is calculated every 10 mm (dx) along the membrane length.

## 4. Results and discussion

### 4.1. Required membrane length

Fig. 5 shows the relationship between A values and required membrane lengths for each recovery rate in the case of $MgCl_2$ concentration of 18.0%. The required membrane length decreases with increase the A value, and converges to almost zero. From this result, increase of an A value reduces required membrane length without any CP.

With ECP condition, the relationship between A values and required membrane lengths for each recovery rate is shown in Fig. 6. Although the required membrane length decreases with increase the A value as same as non-CP condition, required membrane length has converged to the constant values for each concentration and recovery rate, which does not change against any increase A values.

The relationship required A values and membrane lengths with each concentration is shown in Fig. 7, where the target recovery rate is 35%. Even if the given A value is same, the converged membrane length is shortened accompanied with higher concentration.

For more detail consideration, the OP profile with ECP is plotted against the membrane length with the differences of the A values in Fig. 8. The convergence membrane length does not change from the certain value even if the A value increases. This phenomenon is so-called "osmotic equilibrium state". Under ECP condition, though the water flux between FS and DS side increases due to the enhancement of A values,

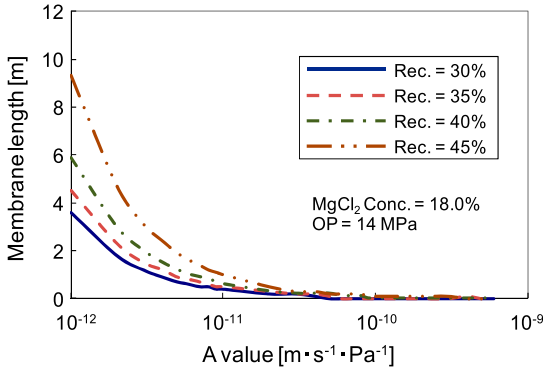


Fig. 5. The relationship between A values and required membrane lengths for each recovery rate. This figure is in the condition of non-CP.

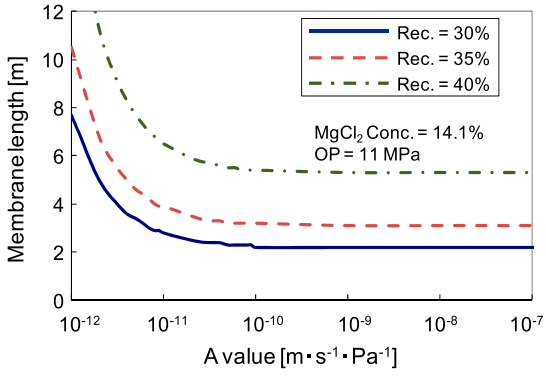


Fig. 6. The relationship between A values and required membrane lengths for each recovery rate. This figure is in the condition of ECP.

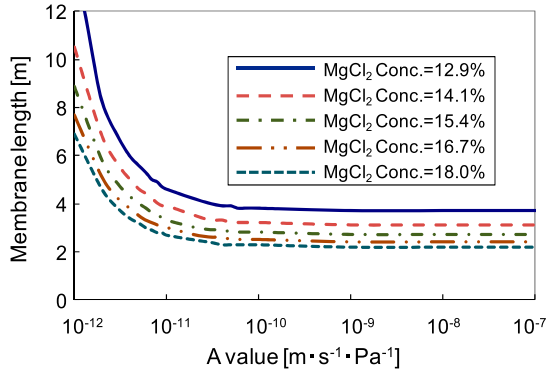


Fig. 7. The comparison between A values and required membrane lengths for each recovery rate of 35%. This figure is in the condition of ECP.

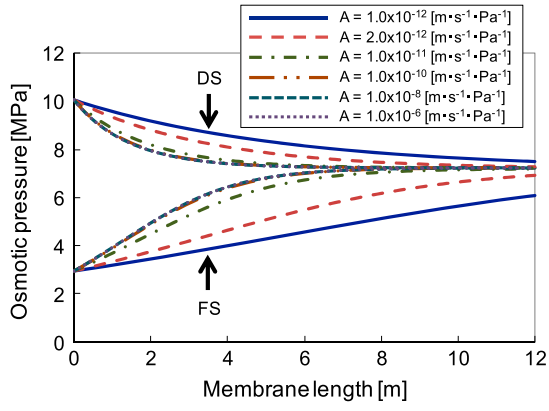


Fig. 8. The osmotic pressure profiles of DS and FS sides along with membrane lengths for each values in ECP condition.

net flux does not change. Namely, the observed flux from FS to DS side does not increase because of osmotic equilibrium, and minimum A value does exist for each condition.

These results indicate that it might be useless developing FO membranes which have A value higher than the required value. The important thing is to develop the FO membrane with minimum A value to obtain the convergence membrane length, and an excess A value does not contribute to decrease the number of membrane elements required or increase the flow rate.

### 4.2. The design direction of FO processes for each recovery rate

Fig. 9 shows the relationship between A values and recovery rates for each number of elements in the case of $MgCl_2$ concentration of 14.1%. Here, the phrase "the number of elements (membrane elements)" not "the membrane length" has to be used, because the unit of the membranes must be natural numbers in the actual process. As mentioned above, the achievable maximum recovery rate is determined by the certain A value regardless of the number of elements.

Achievable maximum recovery rate and the required A value depending on the number of elements, where the $MgCl_2$ concentration is of 12.9 wt% shown in Fig. 10. It starts to converge to the achievable maximum recovery rate at 6 or 7 membranes, and becomes stable over 8 elements. To achieve the maximum recovery rate with 8 elements, the A value of "$2.0 \times 10^{-11}$ [m s$^{-1}$ Pa$^{-1}$]" is required. Therefore, in the case of $MgCl_2$ concentration of 12.9 wt% (the OP is 10 MPa), the FO membranes are required to have the A value over $2.0 \times 10^{-11}$ [m s$^{-1}$ Pa$^{-1}$], while the number of elements is equal to 8 to achieve the maximum recovery rate.

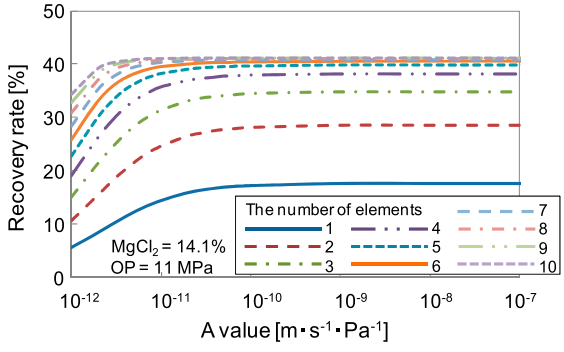


Fig. 9. The relationship between A values and recovery rate of each number of elements.

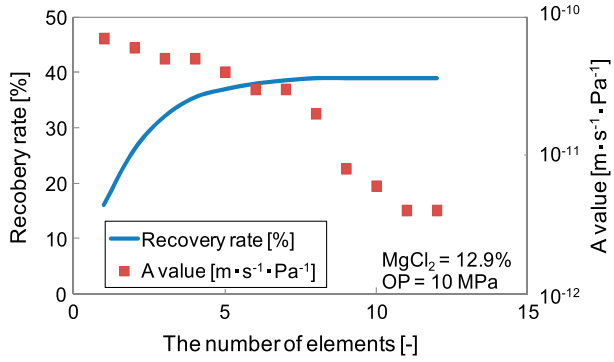


Fig. 10. The comparison of both recovery rate and A values against the number of elements.

As this case, it is possible to calculate the minimum A value and the number of elements at the given concentration of the DS. The calculated results of each concentration are listed in Table 2.

### 4.3. The effect of mass transfer coefficient

Until previous section, $MgCl_2$, one of the common multivalent ionic materials, has been discussed as only DS. However, there is high possibility of using other various DSs in the actual plants. The mass transfer coefficient of DS ($k_D$) varies for each DS. In this section, the effect of $k_D$ difference on the estimation of A values and the number of elements is investigated to generalize the DS.

The case has been assumed for the $k_D$ of $MgCl_2$ with ten times and one tenths from the original value shown in Table 2, when the OP of DS is given as 10 MPa which corresponds to the $MgCl_2$ concentration of 12.9 wt%. This assumption is only applied to three dissociable ionic materials such as

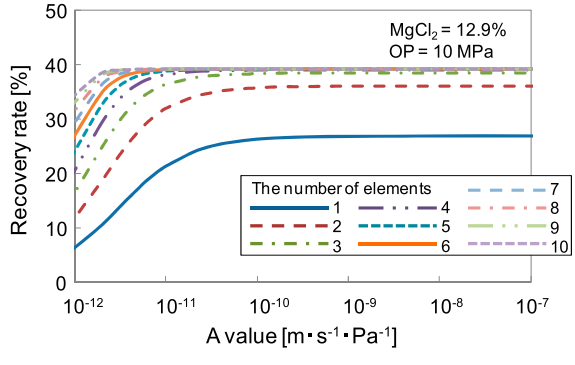


Fig. 11. The relationship between A values and recovery rate of each number of elements in the case of $k_D = 2.76 \times 10^{-4}$[m s$^{-1}$]. This figure is evaluated to determine the effect of the mass transfer coefficient of DS.

$MgCl_2$ ($MgCl_2 \rightarrow Mg^{2+} + 2Cl^-$). In the case of other types of ionic materials and non-ionic materials, the same calculation method can be easily used by changing the calculation condition, because the OP is proportional to the concentration based on the van't Hoff law as mentioned above.

The result of the $k_D$ of $MgCl_2$ with 10 times ($k_D = 2.76 \times 10^{-4}$ [m s$^{-1}$]) is described in Fig. 11. The achievable maximum recovery rate is 39%, where the required A value and the number of elements is $3.0 \times 10^{-11}$ [m s$^{-1}$ Pa$^{-1}$] and 5, respectively. This result suggests that it is possible to estimate the required A value and the number of elements with any DS with different $k_D$ values.

## 5. Conclusion

It is suggested that the external CP has a large effect on the FO membrane performance. A value has a minimum limitation for each condition, that is, the minimum A value exists for the required recovery rate and membrane length. Therefore, the minimum A value and number of elements will be determined if the OP of the DS and the target recovery rate are fixed. It may be useless to develop FO membranes which have higher A values more than required minimum values.

The FO membranes and processes have to be designed by the theoretical approach, and it is possible to make their design direction by applying the theoretical estimation described in this paper.

It is under consideration to improve this approach by taking internal CP into the discussion or by improving the flow condition in the element such as the counter flow. These investigations will be reported in near future.

### Nomenclature

| | | |
|---|---|---|
| A | — | pure water permeability [m s$^{-1}$ Pa$^{-1}$] |
| B | — | solute permeability [m s$^{-1}$] |
| C | — | concentration [mol m$^{-3}$] |
| D | — | diffusion coefficient [m$^2$ s$^{-1}$] |
| $d$ | — | diameter [m] |
| $J_S$ | — | solute flux [mol m$^{-2}$ s$^{-1}$] |
| $J_V$ | — | volumetric flux [m s$^{-1}$] |
| $k$ | — | mass transfer coefficient [m s$^{-1}$] |
| $n$ | — | number of moles [–] |
| $P$ | — | pressure [Pa] |
| $R$ | — | gas constant (= 8.31) [J mol$^{-1}$ K$^{-1}$] |
| $Re$ | — | Reynolds number [–] |
| $Sc$ | — | Schmidt number [–] |
| $Sh$ | — | Sherwood number [–] |
| $T$ | — | absolute temperature [K] |
| $u$ | — | flow velocity [m s$^{-1}$] |
| $V$ | — | volume [m$^3$] |
| $\mu$ | — | viscosity of solution [kg m$^{-1}$ s$^{-1}$] |
| $\nu$ | — | kinematic viscosity [m$^2$ s$^{-1}$] |
| $\pi$ | — | osmotic pressure [Pa] |
| $\rho$ | — | density of solution [kg m$^{-3}$] |

### Subscript

| | | |
|---|---|---|
| b | — | bulk solution |
| D | — | at the draw solution side |
| F | — | at the feed side |
| m | — | membrane surface |
| p | — | permeate |

## References


[1] Global Water Intelligence, IDA Desalination Yearbook 2012–2013, Media Analytics Ltd., Oxford, 2012.

[2] Global Water Intelligence, Global Water Market 2011, Media Analytics Ltd., Oxford, 2010.

[3] Ministry of Economy, Trade and Industry, 2010, Future Vision and Policy Response toward Water Business Industry. Available from <http://www.meti.go.jp/english/policy/mono_info_service/water_business>, accessed August 8, 2013.

[4] Global Water Intelligence, Water Desalination Report 49(14) 2013.

[5] Q. Schiermeier, Purification with a pinch of salt, Nature 452(7185) (2008) 260–261.

[6] M. Elimelech, Yale constructs forward osmosis desalination pilot plant, Mem. Technol. 2007(1) (2007) 7–8.

[7] R.L. McGinnis, M. Elimelech, Energy requirements of ammonia-carbon dioxide forward osmosis desalination, Desalination 207(1–3) (2007) 370–382.

[8] N.A. Thompson, P.G. Nicoll, Forward osmosis desalination: A commercial reality, IDA World Congress 2011, Perth, 2011.

[9] P. Nicoll, Forward osmosis is not to be ignored, Desalin.Water Reuse (February–March) 2 (2013) 30–33.

[10] K. Lampi, Forward osmosis—Business relevant solutions for a growing market, The 3rd Osmosis Membrane Summit, Barcelona, 2012.

[11] M.I. Dova, K.B. Petrotos, H.N. Lazarides, On the direct osmotic concentration of liquid foods: Part II. Development of a generalized model, J. Food Eng. 78 (2) (2007) 431–437.

[12] J.R. McCutcheon, M. Elimelech, Influence of membrane support layer hydrophobicity on water flux in osmotically driven membrane processes, J. Mem. Sci. 318(1–2) (2008) 458–466.

[13] T.Y. Cath, A.E. Childress, M. Elimelech, Forward osmosis: Principles, applications, and recent developments, J. Mem. Sci. 281(1–2) (2006) 70–87.

[14] K.Y. Wang, R.C. Ong, T.S. Chung, Double-skinned forward osmosis membranes for reducing internal concentration polarization within the porous sublayer, Ind. Eng. Chem. Res. 49(10) (2010) 4824–4831.

[15] N.Y. Yip, A. Tiraferri, W.A. Phillip, J.D. Scheffman, M. Elimelech, High performance thin-film composite forward osmosis membrane. Environ. Sci. Technol. 44(10) (2010) 3812–3818.

[16] S. Zhang, K.Y. Wang, T.S. Chung, H. Chen, Y.C. Jean, G. Amy, Well-constructed cellulose acetate membranes for forward osmosis: Minimized internal concentration polarization with an ultra-thin selective layer, J. Mem. Sci. 360(1–2) (2010) 522–535.
[17] M. Sairam, E. Sereewatthanawut, K. Li, A. Bismarck, A.G. Livingston, Method for the preparation of cellulose acetate flat sheet composite membranes for forward osmosis—Desalination using $MgSO_4$ draw solution, Desalination 273(2–3) (2011) 299–307.
[18] N.T. Hancock, T.Y. Cath, Solute coupled diffusion in osmotically driven membrane processes, Environ. Sci. Technol. 43(17) (2009) 6769–6775.
[19] S. Phuntsho, H.K. Shon, S. Hong, S. Lee, S. Vigneswaran, A novel low energy fertilizer driven forward osmosis desalination for direct fertigation: Evaluating the performance of fertilizer draw solutions, J. Mem. Sci. 375(1–2) (2011) 172–181.
[20] J.R. McCutcheon, R.L. McGinnis, M. Elimelech, A novel ammonia-carbon dioxide forward (direct) osmosis desalination process, Desalination 174(1) (2005) 1–11.
[21] J.R. McCutcheon, R.L. McGinnis, M. Elimelech, Desalination by ammonia–carbon dioxide forward osmosis: Influence of draw and feed solution concentrations on process performance, J. Mem. Sci. 278(1–2) (2006) 114–123.
[22] S. Kimura, S. Sourirajan, Analysis of data in reverse osmosis with porous cellulose acetate membranes used, AIChE J. 13(3) (1967) 497–503.
[23] S. Nakao, T. Nomura, S. Kimura, Characteristics of macromolecular gel layer formed on ultrafiltration tubular membrane, AIChE J. 25(4) (1979) 615–622.
[24] S. Nakao, S. Kimura, Analysis of solutes rejection in ultrafiltration, J. Chem. Eng. Jpn. 14(1) (1981) 32–37.
[25] Y. Sato, T. Tsuru, S. Nakao, Model analysis of separation performance of commercial nanofiltration membranes improved by tannic acid, J. Chem. Eng. Jpn. 42 (2) (2009) 95–106.
[26] G. Schock, A. Miquel, Mass transfer and pressure loss in spiral wound modules, Desalination 64(1987) 339–352.
[27] A. Achilli, T.Y. Cath, A.E. Childress, Power generation with pressure retarded osmosis: An experimental and theoretical investigation, J. Mem. Sci. 343(1–2) (2009) 42–52.
[28] Y. Xu, X. Peng, C.Y. Tang, Q.S. Fu, S. Nie, Effect of draw solution concentration and operating conditions on forward osmosis and pressure retarded osmosis performance in a spiral wound module, J. Mem. Sci. 348(1–2) (2010) 298–309.
[29] B. Gu, D.Y. Kim, J.H. Kim, D.R. Yang, Mathematical model of flat sheet membrane modules for FO process: Plate-and-frame module and spiral-wound module, J. Mem. Sci. 379(1–2) (2011) 403–415.